1 **Full paper**

2

3 **Title:** Modularity and evolution of flower shape: the role of efficiency, development, and

4 spandrels in *Erica*

5

6 **Authors:** Dieter Reich[1*], Andreas Berger[1*], Maria von Balthazar[2], Marion Chartier[2],

7 Mahboubeh Sherafati[3], Christian P. Klingenberg[4], Sara Manafzadeh[2], Yannick M. Staedler[2]

8

9 **Affiliations:**

10 [1] Department of Botany and Biodiversity Research, Division of Evolutionary and Systematic

11 Botany, University of Vienna, Rennweg 14, 1030 Vienna, Austria

12 [2] Department of Botany and Biodiversity Research, Division of Structural and Functional

13 Botany, University of Vienna, Rennweg 14, 1030 Vienna, Austria

14 [3] Department of Plant Biology, Faculty of Biological Sciences, Tarbiat Modares University,

15 Tehran, Iran

16 [4] School of Biological Sciences, University of Manchester, Manchester, United Kingdom

17 [*] Equal contribution

18

19 **Corresponding author:** Yannick M. Staedler

20 **Telephone:** +43 1 4277 54084

21 **Email:** yannick.staedler@univie.ac.at

22

23 Word count for the main body of the text: (Introduction, Materials and Methods, Results,

24 Discussion, and Acknowledgements): 5490

25 Word count for Introduction: 1648

26 Word count for Materials and methods: 1032

27 Word count for Results: 1079

28 Word count for Discussion and Conclusion: 1645

29 Word count for Acknowledgements: 65

30

31 Figures: 5 in main text, 3 in supplementary. In colour: Fig. 1, 3, 4, 5, S1, S2, S3

32 Tables: 3 in main text, 10 in supplementary

33 Supporting Information: Methods S1, Notes S1, and Notes S2

34

35 **Summary:**

36 • Three hypotheses can explain floral modularity: the attraction-reproduction, the
37   efficiency, and the developmental hypotheses.

38 • In order to test these hypotheses and understand if pollination specialisation and
39   pollination syndrome influence floral modularity, we focussed on the genus *Erica*: we
40   gathered 3D data from flowers of species with diverse pollination syndromes via
41   Computed Tomography, and analysed their shape via geometric morphometrics. In
42   order to provide an evolutionary framework for our results we tested the evolutionary
43   mode of floral shape, size, and integration under pollination syndrome regimes, and -
44   for the first time- reconstructed the high-dimensional floral shape of their most recent
45   common ancestor.

46 • We demonstrate, for the first time, that the modularity of generalist flowers depends
47   on development and that of specialists is linked to efficiency: in bird syndrome flower,
48   efficiency modules were associated with pollen deposition and receipt, whereas in
49   long-proboscid fly syndrome, they were associated with restricting the access to the
50   floral reward. Only shape PC1 showed selection towards multiple optima, suggesting
51   that PC1 was co-opted by evolution to adapt flowers to novel pollinators. Whole floral
52   shape followed an OU model of evolution, and demonstrated relatively late
53   differentiation.

54 • Flower shape modularity thus crucially depends on pollinator specialisation and class.

55

Introduction:

58 From the bacterial flagellum (McAdams *et al.*, 2004) to the skull shape of dinosaurs (Fabbri *et*

59 *al.*, 2017), modular organisation pervades life's phenotype (Wagner *et al.*, 2007). Modules are

60 subsets of traits that are integrated (i.e. they tend to vary in a coordinated manner) that vary

61 relatively independently from other such subsets (Klingenberg, 2014). Relative independence

62 of modules allows for evolutionary tinkering to take place in one module without much

63 affecting the other (Alon, 2003; Kirsten & Hogeweg, 2011). Modular organisation is thus not

64 only a key feature of the structural complexity of life, but also a key feature for its

65 evolvability (Wagner *et al.*, 2007). Theophrastus' observation, twenty three centuries ago, that

66 "repetition is of the essence of plants" (Theophrastus & Hort, 1916) is underlain by plants'

67 non-conformity to Weissman's doctrine of separation of soma and germ (Weismann, 1892):

68 the indefinite developmental totipotency of meristematic plant cells allows for the modular

69 construction of plants by continuous organogenesis and the repeated production of

70 homologous structures (Herrera, 2009). However, despite the fundamentally modular

71 structure of plants (see Ottaviani et al. 2017 and references therein), historically, most studies

72 of modularity have, and still are, focussed on animals (Klingenberg, 2014; Esteve-Altava,

73 2017)(see Notes S1). In her seminal work, Raissa Berg hypothesised that the variation of

74 traits in specialised flowers is largely uncorrelated with that of vegetative traits (Berg, 1960),

75 i.e. that vegetative and reproductive traits form independent modules, which are themselves

76 highly integrated (Wagner & Altenberg, 1996). Because different floral traits can experience

77 different selection pressures, Berg's hypothesis can be expanded to include modules of traits

78 within the flower (Ordano *et al.*, 2008; Diggle, 2014; Armbruster & Wege, 2018).

79 Accordingly, the following explicit hypotheses of flower modularity have been advanced. The

80 first hypothesis is the *attraction-reproduction modularity hypothesis*; this hypothesis proposes

81 that flowers are divided into a module of attraction comprising the petals and the sepals, and a

82 module of reproduction comprising the stamens and the carpels (Esteve-Altava, 2017), see

83 Fig. **1a**. The second general hypothesis is the *efficiency modularity hypothesis*, which

84 proposes that flowers are divided into a module efficiency that comprises parts from different

85 organs that effect reproduction (constriction of floral tube, pollen sacs of the stamens, stigma

86 of the carpels, etc.), and a module of attraction (e.g. showy part of petals)(Diggle, 2014). This

87 hypothesis has been supported by multiple studies (Herrera, 2001; Fenster *et al.*, 2004;

88 Pigliucci & Preston, 2004; Carvallo & Medel, 2005; Pérez *et al.*, 2007; Bissell & Diggle,

89 2008; Ordano *et al.*, 2008; Bissell & Diggle, 2010; Fornoni *et al.*, 2015; Heywood *et al.*,

90 2017; Armbruster & Wege, 2018). *Efficiency hypotheses* can comprise modules of pollen

3

92   deposition and receipt (see efficiency 1 in Fig. **1b**), or modules involving putative pollinator

93   filters such as corolla aperture (see efficiency 2 in Fig. **1c**).

94   The abovementioned two hypotheses fail to incorporate the specificities of flowers and their

95   fundamental difference from animal structures. Modules in animals are typically searched for

96   on different parts of the same organ, such as the skull (e.g. (Drake & Klingenberg, 2010;

97   Bardua *et al.*, 2019)), the jaw (e.g. (Hulsey *et al.*, 2006)), or the wing (e.g. (Klingenberg *et al.*,

98   2010; Chazot *et al.*, 2016)), whereas flowers are complexes of fundamentally different organs

99   performing fundamentally different functions, such as protection from predators (i.e. sepals),

100   sexual attraction (i.e. petals), male reproduction (i.e. stamens), and female reproduction (i.e.

101   carpels). Moreover, despite their current functional association, these organs have (mostly)

102   evolved from different progenitors and most likely without functional association for ca. 125

103   million years, from the origin of seed plants to that of flowering plants (Morris *et al.*, 2018).

104   We thus propose a third explicit hypothesis of modularity in flowers: *the developmental*

105   *modularity hypothesis* proposes that floral modularity is dominated by developmental factors,

106   i.e. that each organ class (sepal, petal, stamen, and carpel) forms its own module (see Fig. **1d**).

107   The converse of floral modularity, the tendency of groups of features to be independent from

108   each other, is whole-flower integration, the tendency for all the features of the flower to co-

109   vary. Whole-flower integration level has been hypothesised to vary according to pollination

110   system (see below).

111   Flowers are pollinated by organisms that differ greatly in their morphology and sensory

112   systems (see e.g. (Kelber & Jacobs, 2016)). This has led to convergences in the floral

113   morphology of species pollinated by the same group(s) of animals, as described in the

114   pollination syndrome hypothesis (Vogel, 1954; Grant & Grant, 1965; Stebbins, 1970;

115   Johnson, 2006). Syndromes can be divided into specialised syndromes (pollination by one

116   group of pollinators), and generalised syndromes (pollination by several groups of

117   pollinators). In flowers with specialised syndromes, we expect to observe support for different

118   versions of the *efficiency modularity* (see, e.g. (Diggle, 2014)), depending on pollinator class.

119   In generalist flowers, however three main hypotheses have been advanced to explain how

120   pollinators affect floral shape (Aigner, 2001; Sahli & Conner, 2011; Joly *et al.*, 2018), each of

121   which would lead to different floral modules. (1) The "trade-off" hypothesis (Aigner, 2001;

122   Aigner, 2006; Sahli & Conner, 2011) suggests that a change in trait that increases the fitness

123   contribution of one pollinator will decrease the fitness of another. This model predicts that

124   selection by multiple pollinators in multiple directions would cancel each other out, resulting

125   in weak or absent *efficiency modularity*, in which case *developmental modularity* should be

4

126   observed instead. (2) The "trait specialisation" hypothesis (Sahli & Conner, 2011) proposes

127   that individual traits are under selection by a subset of pollinators, resulting in flowers that

128   possess different traits adapted to different pollinators (which predicts several, well-defined

129   *efficiency modules*). (3) The "common shape" hypothesis (Sahli & Conner, 2011) implies that

130   the different pollinators all select for a common shape, which also predicts the existence of

131   *efficiency modules*.

132   Specialisation and pollinator groups have been hypothesised and shown to also influence

133   whole-flower integration (hereafter only referred to as "integration"). That flowers are highly

134   integrated organ complexes has become a paradigm among floral biologists (Stebbins, 1950;

135   Faegri & Van Der Pijl, 1966; Stebbins, 1970; Ordano *et al.*, 2008), as is the hypothesis that

136   specialised flowers are more highly integrated than generalist flowers because specialised

137   pollination is expected to drive the evolution of precise, highly coordinated (integrated) floral

138   traits (Armbruster *et al.*, 1999; Pérez *et al.*, 2007; Rosas-Guerrero *et al.*, 2011; Ellis *et al.*,

139   2014; Gomez *et al.*, 2014; Gomez *et al.*, 2016). Support for this hypothesis has been provided

140   (Meng *et al.*, 2008; Rosas-Guerrero *et al.*, 2011; Gomez *et al.*, 2014); however, support for

141   the opposite hypothesis has unexpectedly also been provided (Armbruster *et al.*, 1999;

142   Edwards & Weinig, 2011; Joly *et al.*, 2018). Moreover, the group of pollinators possibly also

143   determines the magnitude of integration of the flowers (Pérez-Barrales *et al.*, 2007; Gomez *et*

144   *al.*, 2014; Pérez-Barrales *et al.*, 2014; González *et al.*, 2015).

145   Natural selection is an optimising mechanism that increases the accuracy of complex traits,

146   increasing their precision and decreasing their variation (Bell, 1997; Hansen *et al.*, 2006;

147   Gomez *et al.*, 2016). In specialist flowers, floral shape and size should show evidence of

148   stabilising selection around an optimal shape and size adapted to its pollinator, whereas in

149   generalists, the trade-off hypothesis predicts relaxed selection constraints (Johnson & Steiner,

150   2000), and both the trait specialisation hypothesis and the common shape hypothesis (Sahli &

151   Conner, 2011) predict selection similar to that present in specialists. Therefore, from a macro-

152   evolutionary perspective, if floral shape, size, and integration are affected by pollination

153   syndromes, we would expect that within a lineage where a number N of pollination

154   syndromes evolved repeatedly, the evolution of these floral parameters follows a natural

155   selection model such as an Orstein-Uhlenbeck (OU) process with N optima. Alternatively, if

156   floral shape, size, and integration are not affected by pollination syndromes, we would expect

157   that the evolution of these floral parameters follows a drift–like model such as the Brownian

158   Motion (BM) process instead.

159   To our knowledge, no study has yet tested if floral modules change with pollinator groups; if

160   modularity type changes with specialisation, and what the process of evolution of 3D shape,

161   size, and integration in a system with convergent evolution of pollinator systems is. To

162   answer these questions and test these hypotheses requires a study system in which convergent

163   evolution of specialist pollination systems occurred, and that also contains species with

164   generalist pollination; such a system should also possess a constant floral bauplan in order to

165   rigorously homologise structures. *Erica* is such a system: it is a large genus of ca. 800 species

166   mostly distributed in South Africa (Pirie *et al.*, 2016). Within the many South African

167   members of the genus, evolution of pollination via birds and long-proboscid flies (LPF) has

168   possibly repeatedly taken place (Pirie *et al.*, 2011), whereas generalist pollination syndrome

169   has been found to be prevalent in European species (see Table 1). Moreover, the flowers of

170   *Erica* have consistently the same, 4-merous bauplan with mostly 8 stamens (Stevens *et al.*,

171   2004). *Erica* is thus the ideal system to test the effects of pollinator shifts on floral

172   modularity.

173   In order to test the abovementioned modularity and macro-evolutionary hypotheses, we

174   generated 3D models of *Erica* flowers, the shape of which we digitised using geometric

175   morphometric landmarks. We then used this shape dataset to test our different modularity

176   hypotheses in *Erica* flowers (attraction-reproduction, developmental, and efficiency 1 and 2)

177   in flowers with different pollination syndromes. We used phylogenetic reconstructions to test

178   if floral parameters (shape, size, and integration) evolved under selection driven by

179   pollination syndromes or randomly. We thus aim to understand: (1) The relative importance

180   of the components of floral shape and size in predicting pollination syndromes (2) How floral

181   shape modularity changes with pollination syndromes and floral specialisation (3) The

182   possible evolutionary patterns of floral shape in *Erica* (4) The relative roles of natural

183   selection models (i.e. Ornstein-Uhlenbeck) and drift-like models (i.e. Brownian motion) in

184   explaining the evolution of floral shape, size, and integration in respect to pollination

185   syndromes.

186

187   **Materials and Methods**:

188   *Plant material*

189   We analysed ca. 10 flowers each from a single genotype representing nineteen species of

190   *Erica* from the collections of the greenhouses of the Belvedere Garden (Austrian Federal

191   Gardens). We selected species based on their diversity in pollination syndrome (generalist,

192   bird, long-proboscid flies, and wind) and broadly representative phylogenetic position.

6

193   Although limited, our selection contains both older European lineages and species from the

194   more recently diversified and species rich South-Western Cape Clade as defined by (Pirie *et*

195   *al.*, 2011; Pirie *et al.*, 2016), see Method S1 and Table 1 for details.

196   *X-ray tomography*

197   Flowers were contrasted, mounted, and scanned according to (Staedler *et al.*, 2013). See

198   Methods S1 and Table S1 for details.

199   *3D-landmarking & Geometric Morphometrics*

200   Geometric morphometric landmarking was carried out on isosurface models in AMIRA.

201   Thirty-three homologous landmarks were placed on each flower (see Fig. **2a-c**, Table S2).

202   Landmark coordinates were exported as csv-files, concatenated, and imported in MorphoJ

203   1.06d (Klingenberg, 2011). Procrustes fit, and calculation of the covariance matrix, Principal

204   Component Analysis (PCA), modularity analyses, and allometric regressions were performed

205   in MorphoJ. See Methods S1 for details.

206   *Pollination syndrome prediction*

207   Given the scarcity of direct evidence for pollinators of particular *Erica* species, we relied on

208   visitor data, combining published observations of populations in the wild (eight species, see

209   table 1) with our own of individuals in cultivation (one species, see table 1), to assess

210   pollination syndrome. Species with flowers observed to be visited by birds and long-

211   proboscid flies (LPF) (see Table 1) were classified into the specialised bird and LPF

212   syndrome. Wind pollination was documented in one species, which was then classified into

213   the wind syndrome. Species with flowers that were observed to be visited by several groups

214   of insects that could pollinate the flowers were classified into the generalist syndrome. Using

215   these observations, we identified the floral shape and size components discriminating among

216   pollination types using a random forests (RF) classification algorithm (Breiman, 2001). See

217   Methods S1 for details.

218   *Modularity analysis*

219   We used the RV coefficient method of Klingenberg (Klingenberg, 2009), implemented in

220   MorphoJ (Klingenberg, 2011) to test our modularity hypotheses. The methodology uses the

221   RV coefficient, a multivariate generalisation of the squared Pearson coefficient (Escoufier,

222   1973), as a measure of independence of subsets of the landmark data; it identifies sets of

223   landmarks that group together and are likely to function as evolutionary entities. We carried

224   out modularity analyses on subsets of our data pooled by syndrome (variation pooled by

225   species). We then calculated the correlation between the shape variation of the sets of

226   landmarks (RV coefficient) of the partitions corresponding to the *attraction-reproduction*, the

7

227   developmental, and two different efficiency hypotheses (Fig. **1a-d**, table S2) and compared it

228   with that of 100 million random partitions. The proportion of partitions with lower RV

229   coefficient than the tested partition (i.e. partitions showing higher among-set independence)

230   was used as a measure of support for that partition, the lower the proportion, the higher the

231   support (Young, 2006; Gomez *et al.*, 2014).

232   *Estimation of size, and integration*

233   Size was measured as species-level average in centroid size, as implemented in MorphoJ.

234   Integration coefficients were calculated at the species level as shape PCA eigenvalue variance

235   scaled by the total variance and number of variables (Klingenberg & Marugan-Lobon, 2013)

236   as implemented in MorphoJ (see Table S3).

237   *Phylogenetic inference*

238   Phylogenetic relationships were inferred using DNA sequences from two loci of the chloroplast

239   genome (*trn*LF-*ndhJ* and *trnT-L* intergenic spacers) and one loci of the nuclear genome (internal

240   transcribed spacer (ITS)) from 61 pre-existing sequences of 19 *Erica* species as ingroup and

241   *Calluna vulgaris* and *Daboecia cantabrica* as outgroups (see Table S4 for source of the sequences

242   and their GenBank numbers). Divergence time analyses were carried out within a Bayesian

243   framework by employing an uncorrelated lognormal relaxed clock model in BEAST version 1.8.4

244   (Drummond *et al.*, 2012) by applying secondary calibration via using the two previously published

245   nodal ages (Pirie *et al.*, 2016). See Methods S1 for details.

246   *Ancestral Character State Reconstruction*

247   We used a pruned phylogeny (i.e. removing the outgroup) for the 19 *Erica* species included in

248   this study to estimate the probability of the pollination strategy states for all nodes of the

249   phylogeny. As a demonstration of the potential of this approach, we estimated ancestral states

250   of pollination syndromes using Maximum Likelihood (ML) (Harmon *et al.*, 2010; Revell,

251   2012) and empirical Bayes (Revell, 2012) methods. See Methods S1 and Table S5 for details.

252   *Models of floral trait evolution (unidimensional and high-dimensional)*

253   We applied a penalised likelihood approach to high-dimensional phenotypic dataset of flower

254   shapes of 19 *Erica* species to estimate the fit of three different evolutionary models; Brownian

255   Motion (BM), Ornstein–Uhlenbeck (OU), and Early Burst (EB) in order to better understand

256   the process of floral-shape evolution in the clade (Clavel *et al.*, 2018). The analysis was

257   carried out under the *fit_t_pl* function (RPANDA)(Morlon *et al.*, 2016), and the best fit of the

258   abovementioned three models was assessed using the Generalised Information Criterion

259   (GIC) with the *GIC* function (mvmorph)(Clavel *et al.*, 2015). Finally, we employed the

260   parameters derived from the evolutionary model that best fitted our high-dimensional data to

8

261   obtain floral shape reconstructions through time, as implemented in the function *ancestral* and

262   *phyl.pca_pl* (RPANDA)(Morlon et al., 2016). To visualise 3D models of the reconstructed

263   ancestral floral shapes at selected nodes, a 3D surface model of a flower of *Erica hirtiflora*

264   (lying approximatively in the middle of the PC1 x PC2 space plot) was warped to each target

265   ancestral shape. This was carried out by aligning the reconstructed ancestral shape at the

266   selected nodes and the landmark data of the chosen model (*E. hirtiflora*) using a thin plate

267   spline (TPS) interpolation (Wiley et al., 2005), using the function *tps3d* (Morpho)(Schlager,

268   2017) and the function *extractShape* (Clavel *et al.*, 2018).

269   We fitted a series of likelihood models (i.e. Brownian motion and Ornstein-Uhlenbeck

270   models) to understand how changes in pollination syndromes influence the evolution of

271   various continuous unidimensional floral traits of *Erica* (i.e. PC1, PC2, PC3, PC4, PC5,

272   centroid size, and integration). The best fitting model was determined comparing AICc,

273   ΔAICc, and AICc weights among the models. All analyses were implemented using the R

274   package OUwie (Beaulieu *et al.*, 2012). See Methods S1 for details.

275

276   **Results**:

277   *Pollination syndromes prediction*

278   The floral features used in the Random Forest (RF) classification algorithm successfully

279   classified species into pollinator classes. The most important variable for pollinator prediction

280   was tube length (Fig. **S1a**, Tables S6, S7). The next 15 most important variables were

281   landmarks describing the widest and narrowest positions of the corolla, the ovary/style

282   transition, the meeting point of petal lobes, and the position of sepal tips (Fig. **S1a**, Table S6).

283   For 9 of the 10 predicted species, all flowers were assigned to the same pollination syndrome

284   (Table S8). *E. georgica* was classified either as generalist, bird, LPF, or wind syndrome with

285   varying support (Table S8). We assigned *E. georgica* to the LPF syndrome because the tube

286   length of all these flowers corresponds to that syndrome (Fig. **S1b**), and because the shape of

287   the flower and its morphology also corresponds to that syndrome, as defined for *Erica*

288   (Rebelo *et al.*, 1985). Our RF classifications are in agreement with (Rebelo *et al.*, 1985).

289   *Flower shape*

290   Together, principal component (PC) 1 and PC2 account for 62 % of total shape variation

291   (38.9% for PC1 and 22.1% for PC2). The main distortion along the PC1 is a constriction,

292   elongation and slight curving of the corolla tube. Flowers along PC2 are mainly differentiated

293   by the proximal to medial position of the inflation of the corolla. This varies from globose-

294   urceolate to tubular-urceolate flowers along PC1 and cylindrical to ovoid floral shape along

295   PC2. The PC axis-related distortion along PC1 and 2 is visualised by an exemplary shape

296   distortion of a flower of *E. hirtiflora* (Fig. **3**). The spreading along the two axes did not reflect

297   the phylogeny in separating clades defined by (Pirie *et al.*, 2016) (but see the *Evolution*

298   section below). The convergent evolution of bird and LPF syndrome in our dataset display

299   different patterns: the unrelated LPF syndrome flowers are tightly clustered in the

300   morphospace whereas the bird syndrome flowers are in two clusters.

301   *Modularity*

302   In flowers with generalist syndrome, the best supported modularity hypothesis was the

303   *developmental* hypothesis (see Table 2, Fig. **4a**, Fig. **S2a-d**), although the *efficiency*

304   hypotheses 1 and 2 received -weaker- support (see Table 2). In flowers with bird syndrome,

305   the best supported modularity hypothesis was the *efficiency* 1 hypothesis (see Table 2, Fig.

306   **4b**, Fig. **S2e-h**), although the *developmental* hypothesis received –slightly weaker- support

307   (see Table 2). In flowers with LPF syndrome, the best supported modularity hypothesis was

308   the *efficiency* 2 hypothesis (see Table 2, Fig. **4c**, Fig. **S2i-l**), although the *efficiency* hypothesis

309   1 received –weaker- support (see Table 2). In flowers with wind syndrome, the best supported

310   modularity hypothesis was the *developmental* hypothesis (see Table 2, Fig. **4d**, Fig. **S2m-p**).

311   The *attraction-reproduction* hypothesis was not strongly supported for any pollination

312   syndrome (See table 2).

313   *Allometry*

314   The symmetric component of the entire dataset exhibited significant but weak allometry:

315   1.17% & (P = 0.001; see Fig. **S3a**). If the species are split by pollination syndrome, the

316   proportion of variation explained by allometry (pooled by species) differs according to

317   syndrome (see Notes S3). For the sake of brevity, only the allometric deformation in

318   syndromes for which it is both strong (> 10% predicted shape) and significant (P < 0.05) will

319   be discussed here (i.e. long-proboscid flies and wind syndromes). In the flowers with LPF

320   syndrome, large flowers tend to have a more flask-shaped corolla, and the landmarks on the

321   mouth of the corolla are closer to the floral axis (Fig. **S3b**). In the flowers with wind

322   syndrome, large flowers tend to have corolla lobes more open and stamens more exerted (Fig.

323   **S3c**).

324   *Ancestral Character States Reconstruction*

325   Ancestral state reconstruction for pollination syndromes (Fig. **5a**) suggests that the generalist

326   pollination syndrome is the possible most recent common ancestral (MRCA) state in *Erica*.

327   Within our sampled species the bird pollination syndrome, as well as the LPF syndrome

328   evolved twice independently.

329   *Models of floral trait evolution*

330   Under the penalised likelihood approach, the best fitting model to the evolution of the highly-

331   dimensional whole floral shape in *Erica* was the Ornstein–Uhlenbeck model (OU; lowest

332   GIC; Table S9), which assumes evolution towards an optimal floral shape mean as would be

333   expected under selection.

334   The MRCA floral shape of *Erica* most likely displays short and urceolate flowers, as expected

335   for flowers with generalist syndrome (Fig. **5b**, node 1). The reconstructed evolutionary

336   trajectory (under the best fitted model of OU) displays likely late differentiations in flower

337   shape, with most differentiation possibly occurring at the most recent internal nodes of the

338   tree (Fig. **5b**, nodes 3, 7, 8, and 9). In both reconstructed ancestors of convergent evolution of

339   LPF syndrome, the most recent internal nodes (Fig. **5b**, nodes 9 and 11) likely display

340   differentiation but this differentiation is weak compared to that of terminal nodes (Fig. **5b**,

341   flowers of *E. ventricosa*, and *E. georgica*).

342   The results of the fitting of five models (BM_1, BM_S, OU_1, OU_M, and OU_{MV}) on quantitative

343   floral trait evolution (shape PC1-5, size, and integration) under the four pollination-syndrome

344   regimes are summarised in Table 3. The Hessian matrix of one model (i.e. OU_{MV}) displayed a

345   negative eigenvalue for PC3, PC4, integration, and centroid size, which means that this model

346   was too complex for the information contained in these data and it was excluded from the

347   analyses. Different evolutionary scenarios yielded variable AICc distributions, ΔAICc, and

348   AICc weights (see Table 3). The evolution of floral shape along PC1 and centroid size of

349   flowers were found to best fit an OU_M model (see Table 3). This evolutionary model suggests

350   selection around four different optimal values (θ), one per pollination syndrome (see Table

351   S10). This suggests that PC1 and centroid size have different evolutionary means for each of

352   the four pollination syndrome regimes and that there is an evolutionary force that maintains

353   PC1 and size closer to this evolutionary mean than would be expected under a BM model.

354   The evolution of floral shape along PC2, PC5, and floral integration were found to best fit an

355   OU_1 model (see Table 3). This result suggests that there is no difference between the four

356   pollination syndromes, and that PC2, PC5, and integration each evolve towards a single one

357   optimum (θ) across all *Erica* species (Table S10), indicating a lack of evidence for different

358   constraints by the four pollination regimes. The best-fitted model for the evolution of floral

359   shape along PC3 and PC4 was a BM_1 model (see Table 3), where there is no difference

360   between the pollination syndromes, and these floral variables evolve according to a random

361   walk process.

362

11

Discussion:

Modularity

In flowers with the generalist syndrome, our observation of strong support for the *developmental modularity* hypothesis supports the "trade-off" hypothesis of evolution of generalist flowers (which implies the absence of efficiency modules), and invalidates both the "trait specialisation" hypothesis and the "common shape" hypothesis (which both imply the evolution of efficiency modules). This contrasts with flowers with specialised syndromes (bird and LPF syndromes) which display support for (different) *efficiency* hypotheses. Similar patterns of modularity to that supported in flowers with bird syndrome (attraction-receipt-deposition) have been found across angiosperms: in a reanalysis of existing data, the least variable attributes of flowers were found to be those potentially affecting the mechanical fit between flower and pollinator (Cresswell, 1998). The results of (Cresswell, 1998) suggest independence, but do not test for the latter; such a test was carried out only in few studies such as for species of *Nicotiana* (Solanaceae) where such similar efficiency modules (lengths of the floral tube, stamens and gynoecium) were evidenced (Herrera *et al.*, 2002; Bissell & Diggle, 2010).

In the flowers with LFP syndrome, the set of landmarks of the "corolla aperture" does not include any reproductive organs; the function of this set is thus most likely not directly pollen deposition or receipt. In the Cape, flowers with LPF syndrome typically have very narrow floral tubes (Goldblatt & Manning, 2000); *Erica* flowers with this syndrome, however, do not always have narrow tubes, but do have a narrow corolla apertures (see Fig. **4c**) (Rebelo *et al.*, 1985). This corolla aperture likely plays a role in restricting access to the floral rewards to certain classes of pollinators. This interpretation is supported by the allometric shape deformation (how shape changes with size) in LPF syndrome flowers: in shape, in larger flowers the corolla aperture is, relative to the rest of the flower, narrower, but in size, the corolla aperture stays about the same size in smaller and in larger flowers (Fig. **S3b**). Because of its putative function, we propose to refer to the set of landmarks on the corolla aperture as a "restriction module". Similar structures were found to preclude visits from bats in bird-pollinated *Burmeistera* (Campanulaceae), and to vary much less than the rest of the flower (Muchhala, 2006), suggesting they constitute an independent module. Moreover, this restriction module also contains the petal tips (Fig. **4c**), that do not actively contribute to limiting access to the floral reward; their small size relative to the rest of the corolla also precludes a major role in pollinator attraction. Their presence in the restriction module is therefore most likely non-adaptive and only due to their developmental proximity to the

12

397   corolla aperture. Their presence within the restriction module is therefore most likely a

398   spandrel *sensu* Gould and Lewontin (Gould & Lewontin, 1979). If it were feasible, a denser

399   sampling of landmarks across the flowers would probably uncover more of such structures

400   grouping in shape modules owing to their developmental proximity and not their function.

401   In flowers with wind syndrome, support for the developmental hypothesis suggests that the

402   shape of the different organ classes is independent form each other. This could be due to the

403   fact that (1) wind pollinated flowers probably do not require across-organ class modules (for

404   pollen receipt), and (2) that our data is dominated by developmental shape changes.

405   Modelling studies in grasses that have shown that pollen deposition overwhelmingly relies

406   only on direct impact on the stigma and not on air flows generated by the rest of the flower

407   (Cresswell *et al.*, 2010), which suggests that there is no selection pressure for the rest of the

408   flowers to form pollen receipt modules (as in *efficiency* hypothesis 1). The strong but weakly

409   significant allometry reflects typical differences in flower shape related to differences in

410   anthesis stage: larger (older) flowers have more open petals and more exerted stamens than

411   smaller (younger) flowers (Fig. **S3c**); these changes would also cause organs classes to each

412   display shape variation along their own developmental axis and be independent from each

413   other. This notwithstanding, any interpretation is tentative given our limited sampling of this

414   syndrome.

415   *Floral shape evolution*

416   The radiation of *Erica* in the Cape is the greatest known to have occurred there and one of the

417   greatest in recent plant biological history (Pirie *et al.*, 2016). Analyses confirmed the "hotbed"

418   hypothesis in the genus, i.e. that the radiation of *Erica* was due to increased speciation rates,

419   and showed an overall recent slowing down of speciation rates (although they do remain high

420   in the former South Western clade (Pirie *et al.*, 2016)). Shifts in multiple local-scale

421   ecological gradients, and repeated shift in pollinator preferences appear to have taken place

422   (Linder *et al.*, 2010; Pirie *et al.*, 2016). Such a radiation fits Simpson's adaptive zone model in

423   which similar niches become ecologically available to a lineage, free from competitors

424   (Simpson, 1944): when a lineage first enters these zones, phenotypical evolution should at

425   first be fast, but as ecological niches are filled, the rate of phenotypical evolution should then

426   slow down (Simpson, 1944; Schluter, 2000; Losos & Miles, 2002; Harmon *et al.*, 2010). In

427   such a radiation, one would expect to recover an EB mode of phenotypical evolution (Harmon

428   *et al.*, 2010). However, our analysis of the highly-dimensional morphometric dataset of flower

429   shape recovered as the best fit an OU model of evolution (Table S9), a model considered to

430   better represent the importance of selection. This is further supported by our ancestral floral

13

431   shape reconstruction (Fig. **5b**), which indicates a pattern of greater phenotypical variation at

432   the most recent internal nodes of the tree (Figs. 5a & b, nodes 3, 8, 9, 11), a pattern consistent

433   with pollinator-driven selection (OU model (Harmon *et al.*, 2010)). Our finding of strong

434   evolutionary changes over short time scales concurs with previous findings from diverse data

435   sources (Gingerich, 1983; Lynch, 1990; Hendry & Kinnison, 1999; Roopnarine, 2003; Estes

436   & Arnold, 2007; Harmon *et al.*, 2010). This is furthermore strongly supported by our analyses

437   of the evolutionary model of PC1 and centroid size under different regimes (i.e. pollination

438   syndrome) which recovered as best fit an OU_M model of evolution (selection towards

439   different optima; Tables 3, S11), strongly indicating that pollinators have indeed driven the

440   evolution of floral shape (see below), therefore supporting the a strong role for pollinator-

441   driven speciation in *Erica* (Pirie *et al.*, 2011). PC1 corresponds to a shape change from open

442   bell shaped flowers to more elongated, tubular flowers, generating, for the same size, longer

443   tubes and strongly affecting the landmarks on the narrowest and broadest parts of the corolla

444   (see Fig. **3**). These landmarks, together with tube length, were shown by our random forest

445   analyses to be especially important in predicting pollination syndromes (see Table S6). PC1

446   therefore involves a shape change that is especially relevant for the generation of the different

447   floral shapes of the different pollination syndromes. Variation in PC1 was thus most likely co-

448   opted by evolution to generate the different syndrome morphologies, and ended up

449   encapsulating almost 40% of shape variance (Table S10). Similarly, centroid size is strongly

450   correlated with tube length ($R^2 = 0.96$; P= 2.2E-16), the variable we demonstrate to play the

451   strongest role in predicting the different syndromes (Fig. **S1a**, Table S6). Other PCs probably

452   do not generate variation for which divergent selection on syndromes was present (or strong

453   enough to be identified with our limited sampling), and therefore follow either a single

454   optimum (OU_1) or a random model (BM_1) of evolution (Tables 3, S11).

455   Our result, that integration follows an OU_1 model of evolution (selection with a single

456   optimum; Tables 3, S11), does not support increased floral integration in specialist compared

457   to generalist flowers. Our results also contrast with the results of Gomez et al. (2014) who

458   recovered a BM model of evolution for floral integration (Gomez *et al.*, 2014). However,

459   Gomez et al. (2014) included only landmarks placed on the petals (in 2D), whereas our study

460   includes reproductive organs (in 3D). Because, efficiency modularity (including reproductive

461   parts) has been shown to be stronger than attraction modularity (including the petals only)

462   (Rosas-Guerrero *et al.*, 2011), our study likely includes a signal that is not present in that of

463   Gomez et al. (2014). Evolution of whole-flower integration towards a single optimum suggest

464   that evolution of increased integration in functional part of the flowers may come at the cost

14

465   of lower integration with other parts of the flowers, leading to evolution towards a single

466   optimal value in generalised and specialised systems. Our findings thus do not support

467   changes in integration as a whole, but strongly support changes in its structure, an observation

468   congruent with (Ordano *et al.*, 2008).

469

470   **Conclusion:**

471   Our results illustrate for the first time the potential of 3D datasets (that include the

472   reproductive organs of flowers) together with geometric morphometrics to uncover the

473   modularity of the highly dimensional shape of flowers as a function of pollinator syndrome,

474   and together with a novel penalised likelihood framework (Clavel *et al.*, 2018) also for the

475   first time to test the fits of evolutionary models to the macro-evolution of high-dimensional

476   flower shape and reconstruct its trajectory.

477   Simulations of biological evolution have demonstrated that modularity is favoured within

478   environments where selection changes over time in such a way that each new selective

479   pressure shares some of the aspects of the previous selective pressure (Kashtan & Alon, 2005;

480   Kashtan *et al.*, 2007). It has been shown that within a pollination syndrome, selection on floral

481   traits can change from year to year due to fluctuations in pollinator abundance (Herrera, CM,

482   1988; Campbell, 1989; Campbell *et al.*, 1991). We thus speculate that syndromes are such a

483   changing environment, that evolution of a new syndrome is the equivalent to a change of

484   environment, necessitating the evolution of a new modular organisation (although overall

485   floral integration need not change), and finally that fluctuations in pollinator abundance

486   (within a syndrome) play a role in the emergence of flower modularity.

487

494

495

496   **Author contributions:**

497   YS and MvB designed the project, YS and MvB collected the material, DR and AB collected

498   the data and ran preliminary analyses, MC carried out the random forest analyses, SM and MS

499   carried out the phylogenetic analyses, SM carried out the trait evolution analyses, YS and CK

500   carried out the geometric morphometric analyses, SM designed the manuscript, YS and SM

501   wrote the manuscript. DR and AB contributed equally.

502 **Tables:**

503 **Table 1.** Sampling, systematic syndrome, observed (a, b, e-n) or predicted (in the literature: c,

504 d, or via machine learning: RF = Random Forests), and number of flowers scanned.

Species	Clade[a]	Syndrome	Reference	n (flowers)
Erica australis L.	Palearctic	gen	b	11
Erica blandfordia Andrews	Cape	gen	c, RF	11
Erica bolusiae T. M. Salter	Cape	gen	c, RF	10
Erica brachialis Salisb.	Cape	bird	c, j, k	14
Erica capensis T.M. Salter	Cape	gen	c, n	10
Erica curviflora L.	Cape	bird	c, RF	11
Erica georgica L. Guthrie & Bolus	Cape	lpf	RF	15
Erica gracilis J.C. Wendl.	Cape	gen	l	10
Erica hirtiflora Curtis	Cape	gen	c, m	10
Erica lateralis Willd.	Cape	gen	c, d, RF	10
Erica leucotrachela H.A. Baker	Cape	bird	c, RF	10
Erica margaritacea Aiton	Cape	gen	c, RF	13
Erica melanthera L.	Cape	gen	c, RF	10
Erica perspicua J.C. Wendl.	Cape	bird	e, c, g	10
Erica scoparia L.	Palearctic	wind	f	10
Erica spiculifolia Salisb.	Palearctic	gen	RF	12
Erica turgida Salisb.	Cape	gen	c, RF	12
Erica vagans L.	Palearctic	gen	h, i	11
Erica ventricosa Thunb.	Cape	lpf	c, **d**	9

505 Footnote:

506 Visitor data from literature, websites, and personal observation. gen: insect generalist
507 pollination syndrome; LPF: long-proboscid fly. a, (Pirie *et al.*, 2016); b, (Gil-López *et al.*,
508 2014); c, (Rebelo *et al.*, 1985); d, (Rebelo *et al.*, 1984); e, (Heystek *et al.*, 2014); f, (Herrera,
509 J, 1988); g, (Geerts, 2011); h, (Fern & Fern, 2012); i, (Plants_Database, 2019); j, (Turner,
510 2010); k, (Notten, 2012); l, Yannick M. Staedler, pers. obs. on cultivated specimen; m,
511 (Arendse, 2015); n, (Cullinan *et al.*). RF, syndrome predicted via random forests. c and d,
512 contain description of syndromes and attribute different *Erica* species to them. * contains
513 mention of observation for this species.

514

515 **Table 2.** Modularity tests for the *attraction-reproduction*, *developmental*, and *efficiency 1* and

516 *2* hypotheses. (Most significant values in bold).

517

Generalist syndrome

hypothesis	RV of hypothesis	lowest RV	proportion lower RV
Attraction/reproduction	0.22	0.19	1.40E-003
Developmental	0.12	0.11	**2.30E-007**
Efficiency 1	0.13	0.11	4.10E-005
Efficiency 2	0.16	0.14	7.33E-006

Bird syndrome

hypothesis	RV of hypothesis	lowest RV	proportion lower RV
Attraction/reproduction	0.4	0.16	3.50E-002
Developmental	0.19	0.16	3.66E-006
Efficiency 1	0.15	0.14	**3.02E-006**
Efficiency 2	0.29	0.16	3.50E-003

LPF syndrome

hypothesis	RV of hypothesis	lowest RV	proportion lower RV
Attraction/reproduction	0.39	0.3	1.80E-002
Developmental	0.23	0.17	8.07E-004
Efficiency 1	0.17	0.16	4.20E-006
Efficiency 2	0.23	0.22	**5.50E-007**

Wind syndrome

hypothesis	RV of hypothesis	lowest RV	proportion lower RV
Attraction/reproduction	0.72	0.44	2.50E-001
Developmental	0.43	0.32	**1.70E-003**
Efficiency 1	0.47	0.29	4.00E-002
Efficiency 2	0.54	0.34	2.60E-002

518

18

519   **Table 3.** Models of quantitative phenotypic trait evolution (PC1-5 of floral shape, size, and

520   integration) under the pollination syndrome regime, and their biological interpretation, model

521   fit of plausible models for the seven floral variables, indicating AICc (corrected AIC score),

522   ΔAICc, and AICc weight..

523

variables	Model	AICc	DAICc	AICc weight	Interpretation of the best model for shape, integration, and size variable evolution
PC1	BM1	-6.65	7.91	0.015	Evolution of shape along PC1 is constrained;
	BMS	0.46	15.02	4.22E-04	different optima depend on pollination syndromes,
	OU1	-5.5	9.01	0.008	which would imply that optimal shape along PC1
	OUM	**-14.56**	**0**	**0.772**	has evolved separately for different pollination
	OUMV	-11.9	2.66	0.204	syndromes
PC2	BM	-11.31	2.11	0.232	Evolution of shape along PC2 is directed toward
	BMS	-4.76	8.66	0.009	an optimum without being affected by the
	OU1	**-13.42**	**0**	**0.667**	pollination syndromes
	OUM	-9.44	3.98	0.091	
	OUMV	-1.27	12.16	0.002	
PC3	**BM**	**-34.98**	**0**	**0.758**	Evolution of shape along PC3 is random and not
	BMS	-26.25	8.73	0.010	affected by the different pollination syndromes
	OU1	-32.61	2.37	0.231	
	OUM	-22.69	12.29	0.002	
PC4	**BM**	**-38.35**	**0**	**0.630**	Evolution of shape along PC4 is random and not
	BMS	-30.17	8.17	0.011	affected by the different pollination syndromes
	OU1	-37.03	1.32	0.326	
	OUM	-32.5	5.85	0.034	
PC5	BM	-37.62	0.4	0.437	Evolution of shape along PC5 is directed toward
	BMS	-30.49	7.52	0.012	an optimum without being affected by the
	OU1	**-38.01**	**0**	**0.533**	pollination syndromes
	OUM	-31.22	6.8	0.018	
	OUMV	-18.84	19.17	3.66E-05	
Integration	BM	-47.52	1.09	0.364	Evolution of shape integration is directed toward
	BMS	-38.67	9.94	0.004	an optimum without being affected by the
	OU1	**-48.61**	**0**	**0.6264**	pollination syndromes
	OUM	-39.22	9.39	0.006	
Centroid size	BM1	160.28	23.11	9.42E-06	Evolution of size is constrained; different optima
	BMS	144.98	7.81	0.020	depend on pollination syndromes, which would
	OU1	161.09	23.91	6.29E-06	imply that optimal size has evolved separately for
	OUM	**137.17**	**0**	**0.98**	different pollination syndromes

524
525

References

Aigner PA. 2001. Optimality modeling and fitness trade□offs: when should plants become pollinator specialists? *Oikos* **95**(1): 177-184.

Aigner PA. 2006. The evolution of specialized floral phenotypes in a fine-grained pollination environment. *Plant–pollinator interactions: From specialization to generalization* **23**: 46.

Alon U. 2003. Biological networks: the tinkerer as an engineer. *Science* **301**(5641): 1866-1867.

Arendse B. 2015. *Variation in breeding systems and consequences for reproductive traits in Erica.* University of Cape Town.

Armbruster WS, Tuxill JD, Flores TC, Vela JL. 1999. Covariance and decoupling of floral and vegetative traits in nine Neotropical plants: a re□evaluation of Berg's correlation□pleiades concept. *American Journal of Botany* **86**(1): 39-55.

Armbruster WS, Wege JA. 2018. Detecting canalization and intra-floral modularity in triggerplant (Stylidium) flowers: correlations are only part of the story. *Annals of Botany* **123**(2): 355-372.

Bardua C, Wilkinson M, Gower DJ, Sherratt E, Goswami A. 2019. Morphological evolution and modularity of the caecilian skull. *BMC evolutionary biology* **19**(1): 30.

Beaulieu JM, Jhwueng DC, Boettiger C, O'Meara BC. 2012. Modeling stabilizing selection: expanding the Ornstein–Uhlenbeck model of adaptive evolution. *Evolution: International Journal of Organic Evolution* **66**(8): 2369-2383.

Bell G. 1997. *The basics of selection*: Springer Science & Business Media.

Berg RL. 1960. The ecological significance of correlation pleiades. *Evolution* **14**(2): 171-180.

Bissell E, Diggle P. 2010. Modular genetic architecture of floral morphology in Nicotiana: quantitative genetic and comparative phenotypic approaches to floral integration. *Journal of evolutionary biology* **23**(8): 1744-1758.

Bissell EK, Diggle PK. 2008. Floral morphology in Nicotiana: architectural and temporal effects on phenotypic integration. *International Journal of Plant Sciences* **169**(2): 225-240.

Breiman L. 2001. Random forests. *Machine learning* **45**(1): 5-32.

Campbell DR. 1989. Measurements of selection in a hermaphroditic plant: variation in male and female pollination success. *Evolution* **43**(2): 318-334.

Campbell DR, Waser NM, Price MV, Lynch EA, Mitchell RJ. 1991. Components of phenotypic selection: pollen export and flower corolla width in Ipomopsis aggregata. *Evolution* **45**(6): 1458-1467.

Carvallo G, Medel R. 2005. The modular structure of the floral phenotype in Mimulus luteus var. luteus (Phrymaceae). *Revista Chilena de Historia Natural* **78**(4).

Chazot N, Panara S, Zilbermann N, Blandin P, Le Poul Y, Cornette R, Elias M, Debat V. 2016. Morpho morphometrics: shared ancestry and selection drive the evolution of wing size and shape in Morpho butterflies. *Evolution* **70**(1): 181-194.

Clavel J, Aristide L, Morlon H. 2018. A Penalized Likelihood framework for high-dimensional phylogenetic comparative methods and an application to new-world monkeys brain evolution. *Systematic Biology* **68**(1): 93-116.

Clavel J, Escarguel G, Merceron G. 2015. mvMORPH: an R package for fitting multivariate evolutionary models to morphometric data. *Methods in Ecology and Evolution* **6**(11): 1311-1319.

Cresswell J. 1998. Stabilizing selection and the structural variability of flowers within species. *Annals of Botany* **81**(4): 463-473.

575 **Cresswell JE, Krick J, Patrick MA, Lahoubi M. 2010.** The aerodynamics and efficiency of
576   wind pollination in grasses. *Functional Ecology* **24**(4): 706-713.
577 **Cullinan J, Strenberg K, Tribe G**. Simon's Town, Western Cape, South Africa: Ujubee.
578 **Diggle PK. 2014.** Modularity and intra-floral integration in metameric organisms: plants are
579   more than the sum of their parts. *Phil. Trans. R. Soc. B* **369**(1649): 20130253.
580 **Drake AG, Klingenberg CP. 2010.** Large-scale diversification of skull shape in domestic
581   dogs: disparity and modularity. *The American Naturalist* **175**(3): 289-301.
582 **Drummond AJ, Suchard MA, Xie D, Rambaut A. 2012.** Bayesian phylogenetics with
583   BEAUti and the BEAST 1.7. *Molecular biology and evolution* **29**(8): 1969-1973.
584 **Edwards C, Weinig C. 2011.** The quantitative-genetic and QTL architecture of trait
585   integration and modularity in Brassica rapa across simulated seasonal settings.
586   *Heredity* **106**(4): 661.
587 **Ellis AG, Brockington SF, de Jager ML, Mellers G, Walker RH, Glover BJ. 2014.** Floral
588   trait variation and integration as a function of sexual deception in Gorteria diffusa.
589   *Phil. Trans. R. Soc. B* **369**(1649): 20130563.
590 **Escoufier Y. 1973.** Le traitement des variables vectorielles. *Biometrics*: 751-760.
591 **Estes S, Arnold SJ. 2007.** Resolving the paradox of stasis: models with stabilizing selection
592   explain evolutionary divergence on all timescales. *The American Naturalist* **169**(2):
593   227-244.
594 **Esteve☐Altava B. 2017.** In search of morphological modules: a systematic review.
595   *Biological Reviews* **92**(3): 1332-1347.
596 **Fabbri M, Koch NM, Pritchard AC, Hanson M, Hoffman E, Bever GS, Balanoff AM,**
597   **Morris ZS, Field DJ, Camacho J. 2017.** The skull roof tracks the brain during the
598   evolution and development of reptiles including birds. *Nature ecology & evolution*
599   **1**(10): 1543.
600 **Faegri K, Van Der Pijl L. 1966.** *Principles of pollination ecology*. Oxford, UK: Pergman
601   Press.
602 **Fenster CB, Armbruster WS, Wilson P, Dudash MR, Thomson JD. 2004.** Pollination
603   syndromes and floral specialization. *Annu. Rev. Ecol. Evol. Syst.* **35**: 375-403.
604 **Fern K, Fern A 2012**. Erica vagans - L. U.K.: Plants For A Future (Company No. 3204567,
605   Charity No. 1057719).
606 **Fornoni J, Ordano M, Pérez-Ishiwara R, Boege K, Domínguez CA. 2015.** A comparison
607   of floral integration between selfing and outcrossing species: a meta-analysis. *Annals*
608   *of Botany* **117**(2): 299-306.
609 **Geerts S. 2011.** *Assembly and disassembly of bird pollination communities at the Cape of*
610   *Africa.* Stellenbosch: Stellenbosch University.
611 **Gil-López MJ, Segarra-Moragues JG, Ojeda F. 2014.** Population genetic structure of a
612   sandstone specialist and a generalist heath species at two levels of sandstone
613   patchiness across the Strait of Gibraltar. *PloS one* **9**(5): e98602.
614 **Gingerich P. 1983.** Rates of evolution: effects of time and temporal scaling. *Science* **222**:
615   159-162.
616 **Goldblatt P, Manning JC. 2000.** The long-proboscid fly pollination system in southern
617   Africa. *Annals of the Missouri Botanical Garden*: 146-170.
618 **Gomez JM, Perfectti F, Klingenberg CP. 2014.** The role of pollinator diversity in the
619   evolution of corolla-shape integration in a pollination-generalist plant clade.
620   *Philosophical Transactions of the Royal Society B-Biological Sciences* **369**(1649).
621 **Gomez JM, Torices R, Lorite J, Klingenberg CP, Perfectti F. 2016.** The role of pollinators
622   in the evolution of corolla shape variation, disparity and integration in a highly
623   diversified plant family with a conserved floral bauplan. *Annals of Botany* **117**(5):
624   889-904.

625 **González AV, Murúa MM, Pérez F. 2015.** Floral integration and pollinator diversity in the
626   generalized plant-pollinator system of Alstroemeria ligtu (Alstroemeriaceae).
627   *Evolutionary ecology* **29**(1): 63-75.
628 **Gould SJ, Lewontin RC. 1979.** The spandrels of San Marco and the Panglossian paradigm: a
629   critique of the adaptationist programme. *Proceedings of the Royal Society of London.*
630   *Series B. Biological Sciences* **205**(1161): 581-598.
631 **Grant V, Grant KA. 1965.** Flower pollination in the Phlox family.
632 **Hansen TF, Carter AJ, Pélabon C. 2006.** On adaptive accuracy and precision in natural
633   populations. *The American Naturalist* **168**(2): 168-181.
634 **Harmon LJ, Losos JB, Jonathan Davies T, Gillespie RG, Gittleman JL, Bryan Jennings
635   W, Kozak KH, McPeek MA, Moreno☐Roark F, Near TJ. 2010.** Early bursts of
636   body size and shape evolution are rare in comparative data. *Evolution: International*
637   *Journal of Organic Evolution* **64**(8): 2385-2396.
638 **Hendry AP, Kinnison MT. 1999.** Perspective: the pace of modern life: measuring rates of
639   contemporary microevolution. *Evolution* **53**(6): 1637-1653.
640 **Herrera CM. 1988.** Variation in mutualisms: the spatiotemporal mosaic of a pollinator
641   assemblage. *Biological Journal of the Linnean Society* **35**(2): 95-125.
642 **Herrera CM. 2001.** Deconstructing a floral phenotype: do pollinators select for corolla
643   integration in Lavandula latifolia? *Journal of evolutionary biology* **14**(4): 574-584.
644 **Herrera CM 2009.** Multiplicity in unity: plant subindividual variation and interactions with
645   animals. University of Chicago Press, 1-4.
646 **Herrera CM, Cerdá X, Garcia M, Guitián J, Medrano M, Rey PJ, Sánchez☐Lafuente A.
647   2002.** Floral integration, phenotypic covariance structure and pollinator variation in
648   bumblebee☐pollinated Helleborus foetidus. *Journal of evolutionary biology* **15**(1):
649   108-121.
650 **Herrera J. 1988.** Pollination relationships in southern Spanish Mediterranean shrublands. *The*
651   *Journal of Ecology*: 274-287.
652 **Heystek A, Geerts S, Barnard P, Pauw A. 2014.** Pink flower preference in sunbirds does
653   not translate into plant fitness differences in a polymorphic Erica species.
654   *Evolutionary ecology* **28**(3): 457-470.
655 **Heywood JS, Michalski JS, McCann BK, Russo AD, Andres KJ, Hall AR, Middleton
656   TC. 2017.** Genetic and environmental integration of the hawkmoth pollination
657   syndrome in Ruellia humilis (Acanthaceae). *Annals of Botany* **119**(7): 1143-1155.
658 **Hulsey CD, de León FG, Rodiles☐Hernández R. 2006.** Micro☐and macroevolutionary
659   decoupling of cichlid jaws: a test of Liem's key innovation hypothesis. *Evolution*
660   **60**(10): 2096-2109.
661 **Johnson SD. 2006.** Pollinator-driven speciation in plants. *Ecology and evolution of flowers*:
662   295-310.
663 **Johnson SD, Steiner KE. 2000.** Generalization versus specialization in plant pollination
664   systems. *Trends in ecology & evolution* **15**(4): 140-143.
665 **Joly S, Lambert F, Alexandre H, Clavel J, Léveillé☐Bourret É, Clark JL. 2018.** Greater
666   pollination generalization is not associated with reduced constraints on corolla shape
667   in Antillean plants. *Evolution* **72**(2): 244-260.
668 **Kashtan N, Alon U. 2005.** Spontaneous evolution of modularity and network motifs.
669   *Proceedings of the National Academy of Sciences* **102**(39): 13773-13778.
670 **Kashtan N, Noor E, Alon U. 2007.** Varying environments can speed up evolution.
671   *Proceedings of the National Academy of Sciences* **104**(34): 13711-13716.
672 **Kelber A, Jacobs GH 2016.** Evolution of color vision. *Human Color Vision*: Springer, 317-
673   354.

674   **Kirsten H, Hogeweg P. 2011.** Evolution of networks for body plan patterning; interplay of
675   modularity, robustness and evolvability. *PLoS computational biology* **7**(10):
676   e1002208.
677   **Klingenberg CP. 2009.** Morphometric integration and modularity in configurations of
678   landmarks: tools for evaluating a priori hypotheses. *Evolution & development* **11**(4):
679   405-421.
680   **Klingenberg CP. 2011.** MorphoJ: an integrated software package for geometric
681   morphometrics. *Molecular Ecology Resources* **11**: 353-357.
682   **Klingenberg CP. 2014.** Studying morphological integration and modularity at multiple
683   levels: concepts and analysis. *Philosophical Transactions of the Royal Society B-*
684   *Biological Sciences* **369**(1649).
685   **Klingenberg CP, Debat V, Roff DA. 2010.** Quantitative genetics of shape in cricket wings:
686   developmental integration in a functional structure. *Evolution: International Journal*
687   *of Organic Evolution* **64**(10): 2935-2951.
688   **Klingenberg CP, Marugan-Lobon J. 2013.** Evolutionary Covariation in Geometric
689   Morphometric Data: Analyzing Integration, Modularity, and Allometry in a
690   Phylogenetic Context. *Systematic Biology* **62**(4): 591-610.
691   **Linder HP, Johnson SD, Kuhlmann M, Matthee CA, Nyffeler R, Swartz ER. 2010.** Biotic
692   diversity in the Southern African winter-rainfall region. *Current opinion in*
693   *environmental sustainability* **2**(1-2): 109-116.
694   **Losos JB, Miles DB. 2002.** Testing the hypothesis that a clade has adaptively radiated:
695   iguanid lizard clades as a case study. *The American Naturalist* **160**(2): 147-157.
696   **Lynch M. 1990.** The rate of morphological evolution in mammals from the standpoint of the
697   neutral expectation. *The American Naturalist* **136**(6): 727-741.
698   **McAdams HH, Srinivasan B, Arkin AP. 2004.** The evolution of genetic regulatory systems
699   in bacteria. *Nature Reviews Genetics* **5**(3): 169-178.
700   **Meng JL, Zhou XH, Zhao ZG, Du GZ. 2008.** Covariance of floral and vegetative traits in
701   four species of Ranunculaceae: a comparison between specialized and generalized
702   pollination systems. *Journal of integrative plant biology* **50**(9): 1161-1170.
703   **Morlon H, Lewitus E, Condamine FL, Manceau M, Clavel J, Drury J. 2016.** RPANDA:
704   an R package for macroevolutionary analyses on phylogenetic trees. *Methods in*
705   *Ecology and Evolution* **7**(5): 589-597.
706   **Morris JL, Puttick MN, Clark JW, Edwards D, Kenrick P, Pressel S, Wellman CH,**
707   **Yang Z, Schneider H, Donoghue PCJ. 2018.** The timescale of early land plant
708   evolution. *Proc Natl Acad Sci U S A* **115**(10): E2274-E2283.
709   **Muchhala N. 2006.** The pollination biology of Burmeistera (Campanulaceae): specialization
710   and syndromes. *American Journal of Botany* **93**(8): 1081-1089.
711   **Notten A 2012**. Erica brachialis Salisb.In PlantZAfrica, Institute SANB. South Africa:
712   Kirstenbosch National Botanical Garden.
713   **Ordano M, Fornoni J, Boege K, Domínguez CA. 2008.** The adaptive value of phenotypic
714   floral integration. *New Phytologist* **179**(4): 1183-1192.
715   **Pérez-Barrales R, Simón-Porcar VI, Santos-Gally R, Arroyo J. 2014.** Phenotypic
716   integration in style dimorphic daffodils (Narcissus, Amaryllidaceae) with different
717   pollinators. *Phil. Trans. R. Soc. B* **369**(1649): 20130258.
718   **Pérez Barrales R, Arroyo J, Scott Armbruster W. 2007.** Differences in pollinator faunas
719   may generate geographic differences in floral morphology and integration in Narcissus
720   papyraceus (Amaryllidaceae). *Oikos* **116**(11): 1904-1918.
721   **Pérez F, Arroyo MT, Medel R. 2007.** Phylogenetic analysis of floral integration in
722   Schizanthus (Solanaceae): does pollination truly integrate corolla traits? *Journal of*
723   *evolutionary biology* **20**(5): 1730-1738.

724   **Pigliucci M, Preston K. 2004.** *Phenotypic integration: studying the ecology and evolution of*
725   *complex phenotypes*: Oxford University Press.
726   **Pirie M, Oliver E, De Kuppler AM, Gehrke B, Le Maitre N, Kandziora M, Bellstedt D.**
727   **2016.** The biodiversity hotspot as evolutionary hot-bed: spectacular radiation of Erica
728   in the Cape Floristic Region. *BMC evolutionary biology* **16**(1): 190.
729   **Pirie MD, Oliver E, Bellstedt DU. 2011.** A densely sampled ITS phylogeny of the Cape
730   flagship genus Erica L. suggests numerous shifts in floral macro-morphology.
731   *Molecular phylogenetics and evolution* **61**(2): 593-601.
732   **Plants_Database 2019**. Cornish Heath (Erica vagans).In Association NG. U.S.A.
733   **Rebelo A, Siegfried W, Crowe A. 1984.** Avian pollinators and the pollination syndromes of
734   selected mountain fynbos plants. *South African Journal of Botany* **3**(5): 285-296.
735   **Rebelo A, Siegfried W, Oliver E. 1985.** Pollination syndromes of Erica species in the south-
736   western Cape. *South African Journal of Botany* **51**(4): 270-280.
737   **Revell LJ. 2012.** phytools: an R package for phylogenetic comparative biology (and other
738   things). *Methods in Ecology and Evolution* **3**(2): 217-223.
739   **Roopnarine PD. 2003.** Analysis of rates of morphologic evolution. *Annual Review of*
740   *Ecology, Evolution, and Systematics* **34**(1): 605-632.
741   **Rosas☐Guerrero V, Quesada M, Armbruster WS, Pérez☐Barrales R, Smith SD. 2011.**
742   Influence of pollination specialization and breeding system on floral integration and
743   phenotypic variation in Ipomoea. *Evolution: International Journal of Organic*
744   *Evolution* **65**(2): 350-364.
745   **Sahli HF, Conner JK. 2011.** Testing for conflicting and nonadditive selection: floral
746   adaptation to multiple pollinators through male and female fitness. *Evolution:*
747   *International Journal of Organic Evolution* **65**(5): 1457-1473.
748   **Schlager S 2017.** Morpho and Rvcg–Shape Analysis in R: R-Packages for geometric
749   morphometrics, shape analysis and surface manipulations. *Statistical shape and*
750   *deformation analysis*: Elsevier, 217-256.
751   **Schluter D. 2000.** *The ecology of adaptive radiation*: OUP Oxford.
752   **Simpson GG. 1944.** *Tempo and mode in evolution*: Columbia University Press.
753   **Staedler YM, Masson D, Schönenberger J. 2013.** Plant tissues in 3D via X-ray
754   tomography: simple contrasting methods allow high resolution imaging. *PloS one*
755   **8**(9): e75295.
756   **Stebbins GL. 1950.** *Variation and evolution in plants*: Geoffrey Cumberlege.; London.
757   **Stebbins GL. 1970.** Adaptive radiation of reproductive characteristics in angiosperms, I:
758   pollination mechanisms. *Annual Review of Ecology and Systematics* **1**(1): 307-326.
759   **Stevens P, Luteyn J, Oliver E, Bell T, Brown E, Crowden R, George A, Jordan G, Ladd**
760   **P, Lemson K 2004.** Ericaceae. *Flowering Plants· Dicotyledons*: Springer, 145-194.
761   **Theophrastus ToE, Hort SA 1916.** Of the parts of plants and their composition. Of
762   classification. *Inquiry Into Plants and Minor Works on Odours and Weather Signs*:
763   Heinemann.
764   **Turner R 2010**. Sunbird Surprise! Surprises in the world of plant pollination. *Full Circle*
765   *Magazine*. U.K.: Full Circle Team. 34.
766   **Vogel S 1954**. Bliitenbiologische Typen als Elemente der Sippengliederung: Fischer—Jena.
767   **Wagner GP, Altenberg L. 1996.** Perspective: complex adaptations and the evolution of
768   evolvability. *Evolution* **50**(3): 967-976.
769   **Wagner GP, Pavlicev M, Cheverud JM. 2007.** The road to modularity. *Nature Reviews*
770   *Genetics* **8**(12): 921-931.
771   **Weismann A. 1892.** *Das Keimplasma: eine theorie der Vererbung*: Fischer.
772   **Wiley DF, Amenta N, Alcantara DA, Ghosh D, Kil YJ, Delson E, Harcourt-Smith W,**
773   **Rohlf FJ, St John K, Hamann B 2005**. Evolutionary morphing. *VIS 05. IEEE*
774   *Visualization, 2005.*: IEEE. 431-438.

775   **Young NM. 2006.** Function, ontogeny and canalization of shape variance in the primate
776   scapula. *Journal of Anatomy* **209**(5): 623-636.

777

778

779   **Figure legends:**

780

781   **Figure 1 Hypotheses.** Modularity hypotheses tested displayed on schematic representation of

782   an *Erica* flower. (a) the *attraction-reproduction* hypothesis proposes that floral organs groups

783   into fertile (stamens and carpel, in red) versus sterile (sepals and petals, in blue) modules. (b)

784   the *efficiency* hypothesis 1 proposes that parts of the flower group in modules directly

785   involved in pollen receipt (joining of the petals and stigma, in red) and deposition (rest of the

786   corolla mouth and stamens, in yellow), and modules that are not (remainder of the flower in

787   blue). (c) the *efficiency* hypothesis 2 proposes that parts of the flower that restrict access to the

788   floral reward (floral neck, in yellow) form a module, that the carpels form a module, and that

789   the rest of the flower also forms a module. (d) the *developmental* hypothesis proposes that

790   parts for the flower group into modules corresponding to their organ identity: sepals (green),

791   petals (blue), stamens (yellow), or carpels (red).

792

793   **Figure 2 Landmarks.** Landmarks used to digitise the shape of *Erica* flowers. (a) on

794   schematic longitudinal section diagramme of an *Erica* flower. (b) on a 3D model of an

795   actinomorphic flower (*E. hirtiflora*). (c) on a 3D model of a zygomorphic flower (*E.*

796   *leucotrachela*).

797

798   **Figure 3 Shape PCA & syndromes.** Two-dimensional ordination plot from a PCA analysis

799   of 33 landmarks and 209 individual flowers of 19 *Erica* species. A representative flower

800   surface-model for each species is plotted next to the dots corresponding to individual flowers

801   of the same species. Colour and shape coding: green-blue circles, generalist syndrome,

802   orange-red squares, bird syndrome, pink and purple triangles long-proboscid fly syndrome,

803   grey crosses, wind syndrome. Closed symbols: observed visitors, open symbols: predicted

804   visitors. Loadings of axes: x-axis PC1: 38.9% of shape variation, y-axis PC2: 22.1% of shape

805   variation. In order to illustrate changes in floral shape associated with PC1 and PC2, a flower

806   from the centre of the morphospace (*E. hirtiflora*) was distorted according to PC1 and PC2

807   and plotted along their respective axes.

808

809   **Figure 4 Modules in *Erica* flowers.** (a) the best supported partition in flowers with generalist

810   syndrome is the *developmental* hypothesis: a 4-fold partition with each organ class forms one

811   module. (b) the best supported partition in the flowers with bird syndrome is the *efficiency*

812   hypothesis 1, where the corolla lobes and the stamen form a putative "pollen deposition

26

813   module", and joining of the upper corolla lobes and the stigma form a putative "pollen receipt

814   module". The third set of landmarks comprises the rest of the flower. (c) the best supported

815   partition in flowers with long-proboscid fly syndrome is the *efficiency* hypothesis 2, where the

816   landmarks on the narrow corolla aperture form a putative "restriction module" that restricts

817   access to the floral reward to only insects with very narrow proboscises. A second set of

818   landmarks is formed by the gynoecium, and a third set of landmarks comprises the rest of the

819   flower. (d) the best supported partition in flowers with wind syndrome the *developmental*

820   hypothesis: a 4-fold partition with each organ class forms one module. Pollinator drawings,

821   originals. Generalists represented by drawing of bee. Character representing the wind: Zephyr

822   from "The birth of Venus" by Sandro Boticelli (ca. 1480).

823

824   **Figure 5 Ancestral state reconstruction for pollination syndromes and floral shape in**

825   ***Erica***. (a) stochastic character mapping of the four pollination syndromes optimised on a

826   chronogram inferred from Bayesian dating. Pie charts at internal nodes indicate the proportion

827   of stochastic mapping from 1000 runs using the Equal Rates (ER) model. (b) ancestral shape

828   reconstruction and reconstructed evolutionary trajectories for six selected species of *Erica*,

829   including species from all four studied pollination syndromes and two convergent evolution

830   of flowers with long-proboscid fly syndrome.

831

832   **Figure S1 Machine learning.** (a) landmark coordinates and tube length sorted by mean

833   accuracy decrease in predicting pollination syndrome via Random Forest (the tube length is

834   the best variable to predict pollination syndrome). (b) tube length (in mm) in studied species.

835

836   **Figure S2 Hypotheses test: RV distributions.** X-axis RV coefficient, y-axis frequency of

837   values. Red arrow indicates the value of the RV coefficient of the modularity hypothesis

838   tested. Left, hypotheses tested, right results of test. a-d tests for species with generalist

839   syndrome. a, test of *attraction-reproduction* hypothesis. b, test for *efficiency* hypothesis 1. c,

840   test for *efficiency* hypothesis 2. d, test for *developmental* hypothesis. e-h tests for species with

841   bird syndrome. e, test of *attraction-reproduction* hypothesis. f, test for *efficiency* hypothesis 1.

842   g, test for *efficiency* hypothesis 2. h, test for *developmental* hypothesis. i-l tests for species

843   with long-proboscid fly syndrome. i, test of *attraction-reproduction* hypothesis. j, test for

844   *efficiency* hypothesis 1. k, test for *efficiency* hypothesis 2. l, test for *developmental* hypothesis.

845   m-p tests for species with wind syndrome. m, test of *attraction-reproduction* hypothesis. n,

846   test for *efficiency* hypothesis 1. o, test for *efficiency* hypothesis 2. p, test for *developmental*

847   hypothesis. Pollinator drawings, originals. Generalists represented by drawing of bee.

848   Character representing the wind: Zephyr from "The birth of Venus" by Sandro Boticelli (ca.

849   1480).

850

851   **Figure S3 Allometry in *Erica* flowers.** (a) allometric plot. x-axis, log centroid size, y-axis

852   shape axis. All 209 individual flowers from all 19 species studied are plotted. Blue to green

853   dots generalist syndrome, orange to red squares bird syndrome, pink and purple triangles

854   long-proboscid fly syndrome, gray crosses wind syndrome. (b) allometric deformation in

855   flowers with long-proboscid syndrome for a change in log centroid size of 0.2. Pink,

856   schematic drawing of smaller flowers, blue schematic drawing of larger flowers. (c)

857   allometric deformation in flowers with wind syndrome for a change in log centroid size of

858   0.2. Pink, schematic drawing of smaller flowers, blue schematic drawing of larger flowers.

859

860   **List of supplementary data:**

861

862   **Table S1.** Species, sample numbers (n) and scanning conditions of *Erica* flowers.

863   **Table S2.** Landmarks used to digitise the shape of *Erica* flowers, and modules to which they

864   belong in the modularity hypotheses tested.

865   **Table S3.** Species-level average values for size and integration.

866   **Table S4.** Genbank accession numbers for nrDNA ITS and cpDNA trnL-F-ndhJ and trnT-L

867   sequence data.

868   **Table S5.** Discrete character mapping models for pollination syndromes.

869   **Table S6.** Main variables mean accuracy decrease of random forest syndrome prediction.

870   **Table S7.** Corolla tube length per flower.

871   **Table S8.** Classification of 114 individual flowers of diverse *Erica* species into the

872   pollination syndromes,

873   **Table S9.** Support values evolutionary models of floral shape evolution.

874   **Table S10.** Summary of the preferred models of evolution for seven phenotypic trait variables

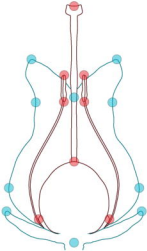875   (PC1-5 of floral shape, centroid size, and integration

876   **Methods S1.** This file contains details of the methodology used to for: X-ray tomography,

877   3D-landmarking, geometric morphometrics, pollination syndrome prediction, modularity

878   analyses (exploratory and confirmatory approaches), phylogenetic inference, ancestral

879   character states reconstruction, and models of trait evolution.

880   **Notes S1.** Literature analysis.

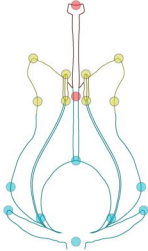881   **Notes S2.** Allometric regressions and correlation between the corolla tube length and centroid

882   size

883   **Scan data.** All the scan data will be deposited on PHAIDRA, the open data repository of the

884   University of Vienna (https://phaidra.univie.ac.at/).

(a) Attraction-reproduction   **(b)** Efficiency 1   **(c)** Efficiency 2   **(d)** Developmental
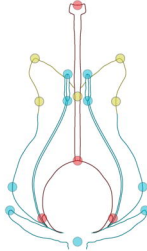
(a)   **(b)**   **(c)**

PC2 and PC1 morphospace plot showing taxa: curviflora, perspicua, leucotrachela, australis, vagans, scoparia, turgida, lateralis, margaritacea, capensis, hirtiflora, spiculifolia, blandifordia, melanthera, bolusiae, georgica, ventricosa, brachialis, gracilis.

(a)   **(b)**   **(c)**   **(d)**

(a)

Erica ventricosa — Long-proboscis fly
Erica lateralis — generalist
Erica leucotrachela — bird
Erica perspicua — bird
Erica curviflora — bird
Erica brachialis — bird
Erica gracilis — generalist
Erica blandfordii — generalist
Erica capensis — generalist
Erica turgida — generalist
Erica hirtiflora — generalist
Erica bolusiae — generalist
Erica melanthera — generalist
Erica georgica — Long-proboscis fly
Erica margaritacea — generalist
Erica australis — generalist
Erica spiculifolia — generalist
Erica vagans — generalist
Erica scoparia — wind

Ma 20   15   10   5   0

(b) Pollination syndrome

Long-proboscis fly
generalist
bird
wind

Erica ventricosa — Long-proboscis fly
Erica lateralis — generalist
Erica leucotrachela — bird
Erica georgica — Long-proboscis fly
Erica melanthera — generalist
Erica scoparia — wind